AIP | Journal of Applied Physics

Investigation of the depolarisation transition in Bi-based relaxor ferroelectrics

David I. Woodward, Robert Dittmer, Wook Jo, David Walker, Dean S. Keeble, Matthew W. Dale, Jürgen Rödel, and Pam A. Thomas

Citation: Journal of Applied Physics **115**, 114109 (2014); doi: 10.1063/1.4869132
View online: http://dx.doi.org/10.1063/1.4869132
View Table of Contents: http://scitation.aip.org/content/aip/journal/jap/115/11?ver=pdfcov
Published by the AIP Publishing

JOURNAL OF APPLIED PHYSICS **115**, 114109 (2014)

Investigation of the depolarisation transition in Bi-based relaxor ferroelectrics

David I. Woodward,[1,a)] Robert Dittmer,[2] Wook Jo,[2] David Walker,[1] Dean S. Keeble,[1] Matthew W. Dale,[1] Jürgen Rödel,[2] and Pam A. Thomas[1]
[1]*Department of Physics, University of Warwick, Coventry CV4 7AL, United Kingdom*
[2]*Institute of Materials Science, Technische Universität Darmstadt, Darmstadt 64287, Germany*

(Received 16 October 2013; accepted 8 March 2014; published online 21 March 2014)

The loss of macroscopic polarisation in relaxor ferroelectric $(Na_{0.8}K_{0.2})_{1/2}Bi_{1/2}TiO_3$ ceramics doped with $BiZn_{1/2}Ti_{1/2}O_3$ has been studied by electrical and structural methods. These indicate that the phenomena that are coupled in a displacive phase transition are not necessarily coupled in the depolarisation of $Na_{1/2}Bi_{1/2}TiO_3$-based relaxors and a concept of correlated and uncorrelated switching of dipoles within adjacent unit cells is used to explain this. Second harmonic generation performed on poled ceramics during heating yields values of the freezing temperature and shows a broad temperature range of ~100 °C across which the structure changes from field-induced ferroelectric to an equilibrium-state ergodic relaxor. Electrical poling at room temperature causes poled regions to increase in size by ~2 orders of magnitude. A model illustrating the main steps in thermal depolarisation is described that does not require a phase transition to take place on a unit cell level. [http://dx.doi.org/10.1063/1.4869132]

I. INTRODUCTION

In the global quest for a lead-free piezoelectric material to replace $Pb(Zr,Ti)O_3$ (PZT), a large number of candidate materials subject to intense research are based on the perovskite $Na_{1/2}Bi_{1/2}TiO_3$ (NBT). NBT is a relaxor ferroelectric[1] as are many of the lead-free piezoelectrics based on NBT.[2]

When a relaxor ferroelectric is cooled below the Burns temperature (T_B), dipoles begin to appear within the unit cells. These dipoles fluctuate between equivalent directions[3] and the relaxor is termed "ergodic."[4] On further cooling, clusters of parallel dipoles tend to form with a size distribution that leads to the frequency dispersion of dielectric permittivity that is the most common indicator of a relaxor ferroelectric. The clusters are of the order of nanometers in size[5] and are referred to as "polar nano-regions" (PNRs). These exist in a matrix of material with randomly oriented dipoles that is macroscopically non-polar.[6,7] Below a freezing temperature, T_F, all polarisation fluctuations are frozen-in and the relaxor is "non-ergodic."[8] A non-ergodic relaxor can be poled by an external electric field, which confers it with long-range order that remains when the field is removed, causing the material to behave as a ferroelectric. When the field-induced structure is heated above T_F, the largest PNRs unfreeze first, with smaller PNRs unfreezing as heating continues. As the dipoles become able to fluctuate, the material returns to being an ergodic relaxor.[4]

At temperatures close to T_F, the macroscopic polarisation of the field-induced material falls to zero. The experimentally obtained depolarisation temperature is referred to as T_d. The temperature range over which this reduction in polarisation occurs can be wide, especially in Bi-based relaxors, hence it has recently been suggested that T_d is best defined as the temperature at which the rate of loss of polarisation is greatest,[9] although a diminished polarisation may persist to higher temperatures.[10] The interactions between individual dipole-dipole pairs are important for describing the behaviour of relaxors,[11] as are interactions between PNRs.[12]

T_d measured by thermally stimulated depolarisation current (TSDC) and dielectric permittivity was compared for the relaxors PLZT 8/65/35 ($Pb_{0.92}La_{0.08}Zr_{0.65}Ti_{0.35}O_3$) and 0.94NBT-0.06BT ($BaTiO_3$).[2] While the two transition temperatures matched almost perfectly in PLZT, T_d obtained from dielectric permittivity was found to be higher than T_d obtained from TSDC for 0.94NBT-0.06BT. This was also observed for several NBT-based materials[9] and for NBT-based materials under an applied electric field,[13,14] leading to the proposal of a transition consisting of two processes; (1) domain randomisation, causing loss of macroscopic polarisation, followed by (2) the break-up of ferroelectric domains into PNRs, causing a change in dielectric behaviour and associated with the transition from field-induced ferroelectric to ergodic relaxor.[15] Neutron[16] and X-ray[17,18] diffraction (XRD) experiments performed on unpoled NBT-based materials do not give unambiguous evidence of a long-range phase transition at temperatures close to T_d and neither have recent birefringence experiments.[19] Subtle changes in XRD peak profiles and the central frequencies of Raman peaks have been observed close to T_d,[18] as have the appearance of nanodomains in electron microscopy[20] that point to a phase transition that takes place without long-range order.

In this work, we focus on the solid solution NBT-KBT ($K_{1/2}Bi_{1/2}TiO_3$). The replacement of Na^+ in NBT with K^+ leads to an increase in the piezoelectric response of the material[21,22] and a decrease in T_d from ~170 °C to ~100 °C.[10,23,24] The composition and temperature-based

a)d.i.woodward@warwick.ac.uk

structural changes are not well known because of the small distortions involved and reports of a wide two-phase region as a function of composition.[25] However, various electrical properties, including the piezoelectric coefficient d_{33}, were found to be maximised at the composition $(Na_{0.8}K_{0.2})_{1/2}Bi_{1/2}TiO_3$.[21] $Bi(Zn_{1/2}Ti_{1/2})O_3$ (BZT), a perovskite with an extremely high spontaneous strain,[26] was found to increase T_d of this composition when used to dope by 2%.[24] This is particularly unusual as T_d is generally found to fall in response to doping of NBT with, for example, BT,[27] $NaNbO_3$, and $KNbO_3$.[23] Substitution by 4% prevented the material from retaining its field-induced polarisation.

Particular use has been made of second harmonic generation (SHG) to give insight into the changes in microstructure that occur as a result of electric poling and temperature. SHG is a technique where the application of high-intensity light from a laser to a dielectric material causes oscillations of the electrons in the structure. As the electric field strength of the laser is similar in magnitude to the local fields within the crystal structure, the relationship between the material polarisation, P, and the electric field of the laser, E, becomes non-linear and requires a Taylor series expansion to be accurately described

$$P = P_0 + \varepsilon_0\chi^{(1)}E + \varepsilon_0\chi^{(2)}E^2 + \varepsilon_0\chi^{(3)}E^3 + \ldots, \quad (1)$$

where P_0 is the spontaneous polarisation of the material, ε_0 is the permittivity of a vacuum, and $\chi^{(n)}$ are the nth order terms of the dielectric susceptibility. As E is a sinusoidally varying function, the second order term contains a component of the polarisation that oscillates at twice the frequency of the laser.[28] The radiation of energy from this component is visible as frequency-doubled light. The higher-order terms contain components of higher harmonics, but these are emitted at intensities typically orders of magnitude less than the second harmonic.[29] The second order dielectric susceptibility, $\chi^{(2)}$, is a third rank tensor and its obligation to be consistent with the crystal symmetry means that for crystals possessing a centre of symmetry, all terms in the matrix are zero. The emission of a second harmonic by a material is therefore strong evidence of a non-centrosymmetric structure, also a prerequisite for the property of piezoelectricity. In the dielectric materials used in this study, with no magnetic elements and no applied field, the origin of the measured second harmonic is structural. When the crystal structure goes through a phase transition that involves the creation of a centre of symmetry, the second harmonic intensity (I_{SH}) falls to zero, providing a simple method of establishing the temperature of a phase transition between ferroelectric and paraelectric states in a classical ferroelectric material. Phase transitions between non-centrosymmetric phases can also be shown.[30,31]

In SHG experiments performed on lead-based relaxors such as PLZT 8/65/35, I_{SH} falls on heating over the temperature range 0–50 °C, associated with macroscopic depolarisation but not with a change in symmetry.[32] I_{SH} also falls to a low but non-zero value as the material changes on heating from the non-ergodic to the ergodic state.[33] T_B was found to be associated with a further reduction in the second harmonic intensity. Similar behaviour has been observed for $Pb(Mg_{2/3}Nb_{1/3})O_3$-based relaxors.[34,35]

SHG performed on Pb-free relaxors in the $Li_xK_{1-x}TaO_3$ series[36,37] demonstrates that samples cooled through T_F under an applied electric field develop values of I_{SH} that are at least an order of magnitude higher than those cooled without a field applied. SHG collected on heating unpoled samples with a consistently applied electric field produces a peak around T_F. Other applications of SHG to Pb-free relaxors are in studying the kinetics of switching in materials such as $Sr_xBa_{1-x}Nb_2O_6$.[38] To the best of our knowledge, the only SHG study on Bi-based relaxors was performed without applied field on single crystals of NBT.[16] This showed the greatest reduction in I_{SH} on heating through ~200 °C, a temperature associated with depolarisation and not with any structural phase transition.

In SHG, an important quantity is the coherence length, l_c, a value which depends on the wavelength of the incident laser and the difference between the refractive indices of the material at the incident and doubled frequencies

$$l_c = \frac{\lambda}{4(n_{2\omega} - n_{\omega})} \quad (2)$$

(l_c = coherence length, λ = wavelength of incident beam, $n_{2\omega}$ = refractive index of particle at second harmonic frequency, and n_{ω} = refractive index of particle at incident frequency).

In order for a strong SHG signal to be measured from a non-centrosymmetric material, it is necessary for the mean particle size to be the same order of magnitude as the coherence length. For samples where the mean particle size $\ll l_c$, there is an approximately linear relationship between I_{SH} and particle size.[39]

In this study, SHG was used to probe the transition between induced ferroelectric and relaxor states and was contrasted to electrical measurements and both bulk and local structural changes.

II. EXPERIMENTAL DETAILS

Two compositions were studied: 0.8NBT–0.2KBT and 0.98(0.8NBT–0.2KBT)–0.02BZT, referred to as 0BZT and 2BZT, respectively. Powders of these two compositions were produced by a conventional solid-state reaction. Na_2CO_3, K_2CO_3, Bi_2O_3, TiO_2, and ZnO (Alfa Aesar, all ≥99% purity) were mixed in stoichiometric quantities for 24 h with zirconia balls and ethanol in a planetary ball mill at 250 rpm. The slurry was dried at 100 °C and the powder was calcined in a lidded alumina crucible for 3 h at 900 °C. The reacted powder was remilled as before and dried, before being ground with a pestle and mortar and sieved. The powder was uniaxially pressed into pellets, which were further pressed under a hydrostatic pressure of 300 MPa and sintered for 3 h at 1100 °C in covered crucibles while covered in powder of the same composition.

Ceramic discs of diameter 7 mm and thickness ~1 mm were prepared by grinding flat, polishing and heating to 400 °C to release mechanically induced strains. Silver paint

was applied to the flat faces for electrodes and ceramics were poled at $5\,kV\,mm^{-1}$. This field is significantly in excess of the coercive field for these materials ($3.1\,kV\,mm^{-1}$ for 0BZT; $3.5\,kV\,mm^{-1}$ for 2BZT).[24] After poling, the piezoelectric coefficients of the materials were the same as those reported in Ref. 24. TSDC was measured at a heating rate of $2\,^{\circ}C\ min^{-1}$ using a Keithley 6517B resistance meter while the sample was heated in a furnace with a small heating chamber. An independent thermocouple confirmed that the temperatures measured were correct to within 2 °C.

High-resolution XRD was performed on pellets poled at $5\,kV\,mm^{-1}$. XRD was performed using a Panalytical X'Pert Pro MPD with a curved Johansson Ge monochromator producing $CuK_{\alpha 1}$ radiation. An Anton Paar HTK1200N furnace was used to heat the samples at a rate of $2\,^{\circ}C\,min^{-1}$ with 5 min dwells before recording data. The temperatures were calibrated against the phase transition in KNO_3 (Ref. 40) giving an accuracy of 2 °C. All peaks are indexed according to the pseudocubic perovskite unit cell.

In the SHG experiments, a Nd-YAG (Yttrium Aluminium Garnet) laser produced a vertically polarised beam of wavelength $\lambda = 1064$ nm. A glass slide was used to split the beam with a small proportion reaching a photodiode to record the intensity of a fraction of the fundamental beam and the majority entering a small furnace in which the ceramic was mounted. The second harmonic exited the furnace through another small hole. A combination of a BG-18 filter with a 35-8465 narrow bandwidth filter (Ealing Inc. CA, USA) placed before a photomultiplier tube suppressed the fundamental beam and all related harmonics with the exception of the second harmonic. The incident and second harmonic beams from both the photodiode and the photomultiplier were displayed on an oscilloscope and recorded on a computer using Labview software (National Instruments, TX, USA). The thermocouple in the furnace was calibrated against the two phase transitions in a ceramic of $K_{1/2}Na_{1/2}NbO_3$ (KNN) giving an accuracy of 5 °C. This allowed the possible effects of sample heating by the laser to be taken into account, although a low power setting was used and no samples showed signs of laser-induced damage after the experiment. An empty sample holder and a sample of centrosymmetric $SrTiO_3$ were both tested and no intensity was recorded, indicating that any first or third harmonics reaching the photomultiplier tube were of insignificant intensity. The intensity of the second harmonic ($\lambda = 532$ nm) was normalised for any fluctuations in the laser intensity by dividing by the square of the intensity of the incident beam.[39] The SHG set-up is depicted elsewhere.[41] Ceramic pellets used for SHG were poled at a range of electric fields, with $5\,kV\ mm^{-1}$ as the maximum for both compositions since larger electric fields resulted in dielectric breakdown of the ceramic. After poling, the silver paint was removed with acetone and the pellet mounted in the furnace with its polarisation direction oriented parallel to the propagation direction of the laser. For temperature-dependent measurements, samples were heated at a rate of $1\,^{\circ}C\,min^{-1}$. To assess any anisotropy in I_{SH} of the ceramic, a bar of 0BZT was cut with dimensions $1\,mm \times 1\,mm \times 10\,mm$, poled between a pair of the 1 mm-spaced faces, placed horizontally in the laser beam and rotated about its long axis (Fig. 1). With this set-up, it was possible to collect I_{SH} as a function of the angle between the laser and sample polarisation vectors to investigate the existence of anisotropy. This was repeated with the sample partially and fully depoled. Partial depoling was achieved by heating the sample at $2\,^{\circ}C\,min^{-1}$ to the indicated temperature for 10 min, followed by cooling at the same rate.

Raman spectroscopy was performed on pellets with a Renishaw inVia Raman Microscope using the 442 nm line of a He-Cd laser as the excitation source, focused to a spot with $\sim 1\,\mu m$ diameter. The laser power at the sample was 20 mW. No damage was suffered by the sample and the Raman spectra did not change over long periods of exposure to the laser. Pellets were placed in a Linkam TS1500EV heating stage and heated at $2\,^{\circ}C\,min^{-1}$. Spectra were then acquired from multiple locations at temperatures of interest. To account for thermal expansion, the laser was re-focused prior to the measurements at each temperature. The sample temperature was calibrated using an additional thermocouple on the pellet surface. Analysis of the resulting spectra was made with Matlab 8.1 software (The Mathworks Inc., MA, USA). The spectra were deconvolved into Gaussian-Lorentzian modes, which were then corrected by the Bose-Einstein factor.

III. RESULTS

A. Electrical properties

The *in-situ* d_{33} data for the two compositions have been measured before[24] and demonstrate that the maximum rate of depolarisation occurs at 100(1) °C for 0BZT and 114(1) °C for 2BZT with the majority of the polarisation lost over a fairly narrow temperature range of ~20 °C. TSDC data in Fig. 2 show that the maximum depolarisation current occurs at 103(1) °C for 0BZT and 119(1) °C for 2BZT, values that are only slightly higher than those obtained from d_{33} measurements.

B. XRD

XRD patterns were obtained from ceramics that were either unpoled or poled at $5\,kV\ mm^{-1}$ (Fig. 3). The scans from

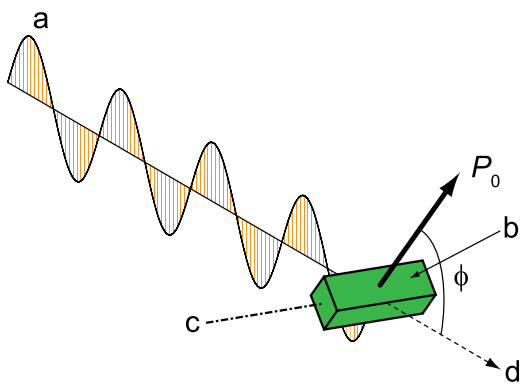

FIG. 1. Diagram illustrating the experimental set-up enabling I_{SH} to be measured as a function of the angle between laser and sample polarisation vectors. (a) Vertically polarised fundamental (infra-red) beam, (b) ceramic sample, (c) axis of sample rotation, and (d) fundamental and second harmonic beams exiting sample.

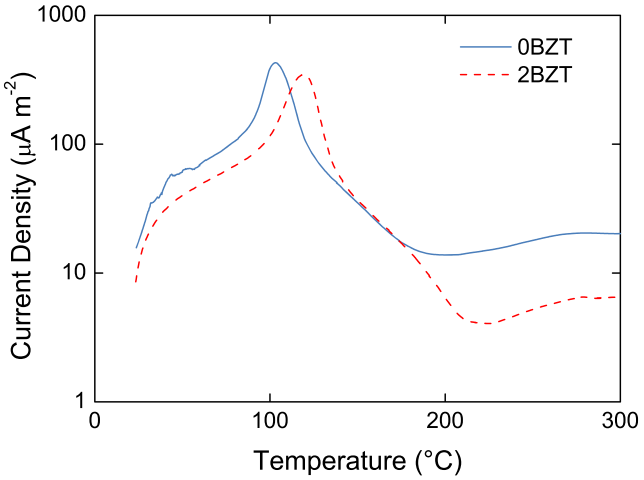

FIG. 2. TSDC for poled 0BZT and 2BZT ceramics.

unpoled samples predominantly feature peaks that are consistent with a pseudocubic structure, although the asymmetry of peak profiles indicates the presence of structural distortions. After poling, peaks are split in a manner consistent with a rhombohedral structure—with the {110} and {111} peaks as doublets and the {100} and {200} peaks as singlets. Strong preferential orientation in poled ceramics makes the {111} peak at high d-spacing have a higher intensity than the {111} peak at lower d-spacing, in contrast to diffraction from rhombohedral materials with no preferential orientation. The act of poling appears to change the pseudocubic material into rhombohedral material; though at the fields used, some pseudocubic material remains, most noticeably in the 0BZT sample. The rhombohedral phase in 2BZT has a larger rhombohedral strain than in 0BZT.

Poled ceramics were heated and XRD patterns collected. Fig. 4 contains contour plots from four of the peaks as a function of temperature. At room temperature, these peaks show the splitting associated with rhombohedral structures. On heating both compositions, the field-induced strain that causes this splitting decreases and the structure becomes pseudocubic. There is no clear displacive transition between these two structures, as might be expected from a classical ferroelectric (e.g., Ref. 42). Instead, the pseudocubic phase

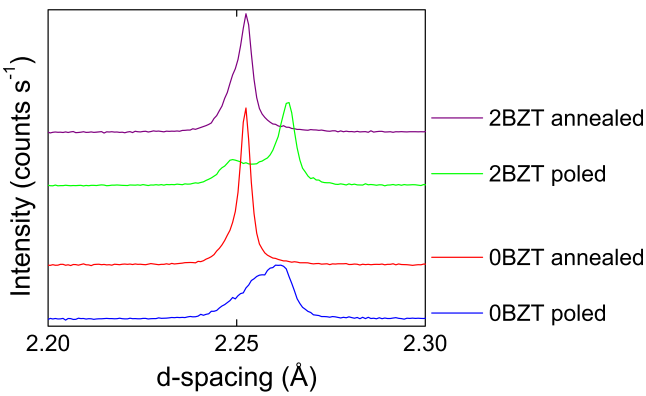

FIG. 3. {111} peak in room-temperature XRD patterns for samples of poled and annealed ceramics for both 0BZT and 2BZT samples. The intensity is plotted on a linear scale.

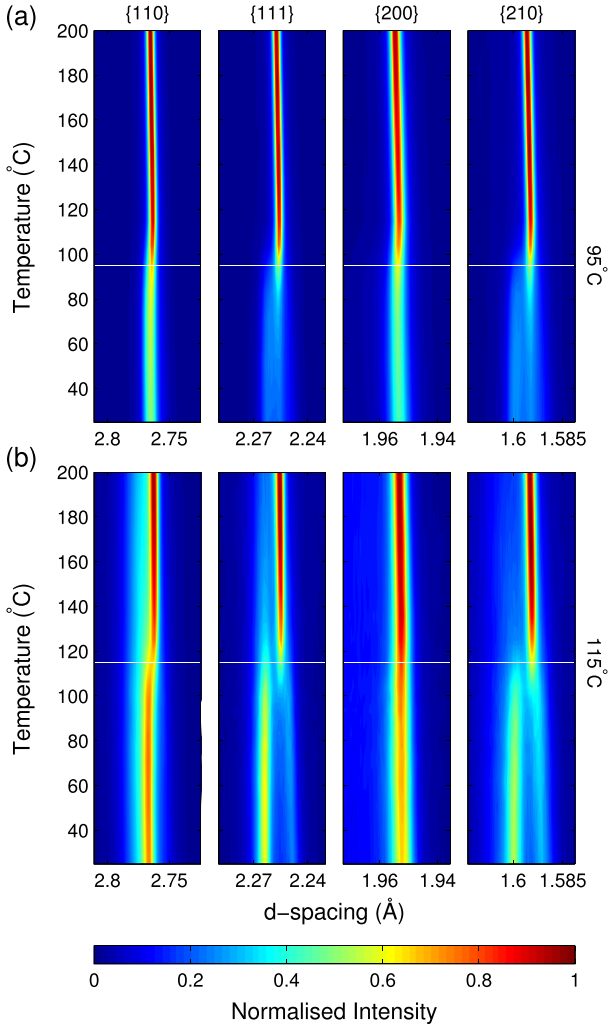

FIG. 4. Contour plots showing the temperature evolution of {110}, {111}, {200}, and {210} XRD peaks obtained from poled ceramics (a) 0BZT and (b) 2BZT.

grows at the expense of the rhombohedral phase. Assigning a transition temperature can be difficult as there is no narrow temperature range in which the rhombohedral phase completely disappears, but the greatest change in the diffraction patterns is observed at 95(2) °C for 0BZT and 115(2) °C for 2BZT. Attempts to refine the proportions of the two phases were unsuccessful because of strong correlation between the scale factors and the thermal parameters.

C. SHG

Unpoled ceramics were found to give weak, but non-zero, second harmonics. However, poling of ceramics led to an increase in I_{SH} of at least an order of magnitude (Fig. 5). On heating, I_{SH} was found to drop sharply as the material depolarised and was not recovered on cooling. Data obtained on cooling appeared the same as data obtained from unpoled ceramics.

The increase in I_{SH} associated with poling is only observed for electric fields that exceed $1\,\mathrm{kV\,mm^{-1}}$, even though a weak d_{33} can be measured after poling at this field. In 0BZT, the value of I_{SH} after poling continues to increase up to the maximum field value, with the greatest increase

found between 3 and 4 kV mm^{-1}. In 2BZT, the value of I_{SH} after poling increases up to 3 kV mm^{-1}, but falls slightly on poling at larger electric fields. The greatest increase in I_{SH} is found between 2.5 and 3 kV mm^{-1}, significantly lower than the coercive field for this material, 3.5 kV mm^{-1} (Ref. 24).

The TSDC and XRD data show a smooth transition from poled to unpoled states. However, the SHG data show a distinct change in gradient at a well-defined temperature. In 0BZT poled at the maximum field strength, this is at 95(5) °C with I_{SH} approaching the unpoled values at around 160(5) °C. In 2BZT poled at the maximum field strength, it is at 130(5) °C and approaches the unpoled values at around 230(5) °C. Notably, I_{SH} for the 2BZT ceramic poled at 2.5 kV mm^{-1} starts to fall at a significantly lower temperature than when it is poled at a higher electric field.

The precise shape of the I_{SH} curve as a function of temperature is dependent on many factors, including thermal history, residual stresses, and damage sustained by arcing during poling. In particular, we have observed a saw-tooth appearance in I_{SH} for ceramics that have suffered mechanical stresses such as grinding with abrasive paper. Annealing at a suitably high temperature removes these oscillations. In these data (Fig. 5), the oscillations appear most clearly in 2BZT poled at 5 kV/mm and may indicate that poling has generated significant stresses in the material.

I_{SH} of an unpoled ceramic at a fixed temperature is isotropic with respect to its orientation relative to the fundamental beam and is affected only by the geometry of the sample. In a poled ceramic, it is possible for anisotropy in I_{SH} to be observed if the angle between the sample polarisation and the polarisation direction of the laser beam is allowed to vary (Fig. 1). The data in Fig. 6 show the change in I_{SH} of a poled ceramic bar with a square cross-section, in both unpoled and fully poled (5 kV mm^{-1}) states, in addition to the same bar partially depoled by consecutive heating to 120 and 125 °C.

I_{SH} from the unpoled (isotropic) sample undergoes variation purely due to sample geometry; a cylindrical sample would have reduced this variation to zero, but it was necessary to maintain a square cross-section in order to pole the material with a uniform field. I_{SH} from the poled sample has increased in all directions and yet shows the same dependence on ϕ as the unpoled sample. This indicates that, at all states of poling, the 0BZT ceramic generates the second harmonic isotropically and no further angle-dependent analysis need be performed.

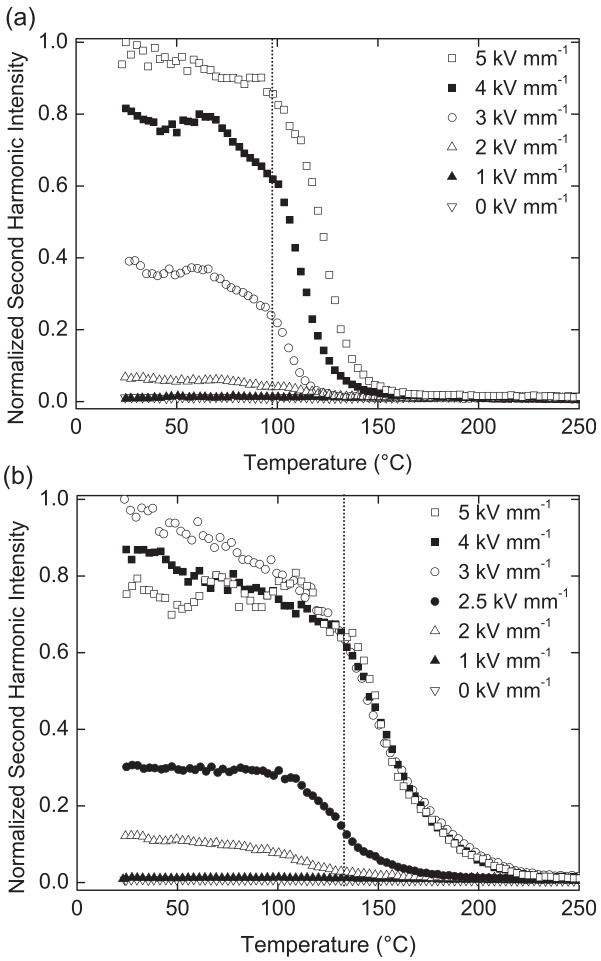

FIG. 5. I_{SH} for (a) 0BZT and (b) 2BZT ceramics, poled at a range of electric field strengths. Data are normalized to the maximum value measured for each material. The dotted line in each graph indicates the temperature at which the gradient of I_{SH} changes most sharply for the samples poled at high field strengths; 95(5) °C for 0BZT and 130(5) °C for 2BZT.

D. Raman spectroscopy

Raman spectra collected for both samples (Fig. 7) were found to exhibit similar profiles to those collected for NBT,[18] and rhombohedral modifications of NBT-KBT[43] and NBT-BT.[44] The mode observed at ~520 cm^{-1} was assigned by Kreisel *et al.*,[45] to an A_1 transverse optic mode originating from vibrations of the TiO_6 octahedra. Studies of relaxor perovskite systems such as $Ba(Ti_{0.7}Sn_{0.3})O_3$ (Ref. 46) and $Ba(Ti_{0.6}Zr_{0.4})O_3$ (Ref. 47) have shown that the intensity of this mode falls as the sample is heated above T_F, approaching zero at T_B. Fig. 8 indicates the change in the intensity of this mode on heating for both samples. These data reveal a slight increase in intensity at 90(10) °C, close to the expected value of T_d, that was found to be repeatable for both samples. A continuous reduction in intensity is observed across the

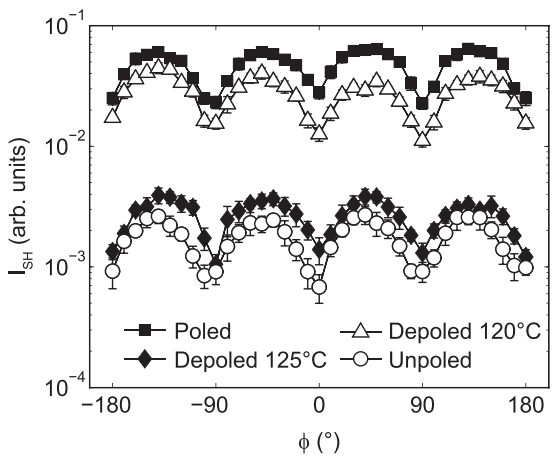

FIG. 6. I_{SH} measured as a function of the angle ϕ between the laser and sample polarisation vectors for 0BZT poled at 5 kV mm^{-1}, partially depoled by heating to 120 °C, partially depoling by heating to 125 °C and unpoled. I_{SH} values are plotted on a log scale.

range 150–400 °C, indicating that PNRs are shrinking continuously, as observed in other lead-based[48] and lead-free[46,47] relaxor systems.

IV. DISCUSSION

In unpoled non-ergodic relaxors, the PNRs may be viewed as nano-scale particles in a non-polarised matrix. In SHG, the use of an infrared laser gives l_C in the much larger region of ~1 μm (Ref. 49) and the result is that I_{SH}, linearly dependent on the particle size, is very weak. On poling with an electric field strength of 5 kV mm^{-1}, I_{SH} increases by around an order of magnitude. If this increase in I_{SH} was due to the realignment of dipoles in an arrangement that strongly favoured the production of the second harmonic in a particular crystallographic orientation, then it would be expected that I_{SH} would be weaker at different orientations. The data in Fig. 6 indicate that this is not the case and so it is proposed that the difference in I_{SH} between poled and unpoled samples (Figs. 5 and 6) is as a result of poling, causing the growth of poled regions across the sample, analogous with domains in a classical ferroelectric and that I_{SH} is linked to the size of these regions, rather than the macroscopic polarisation value.

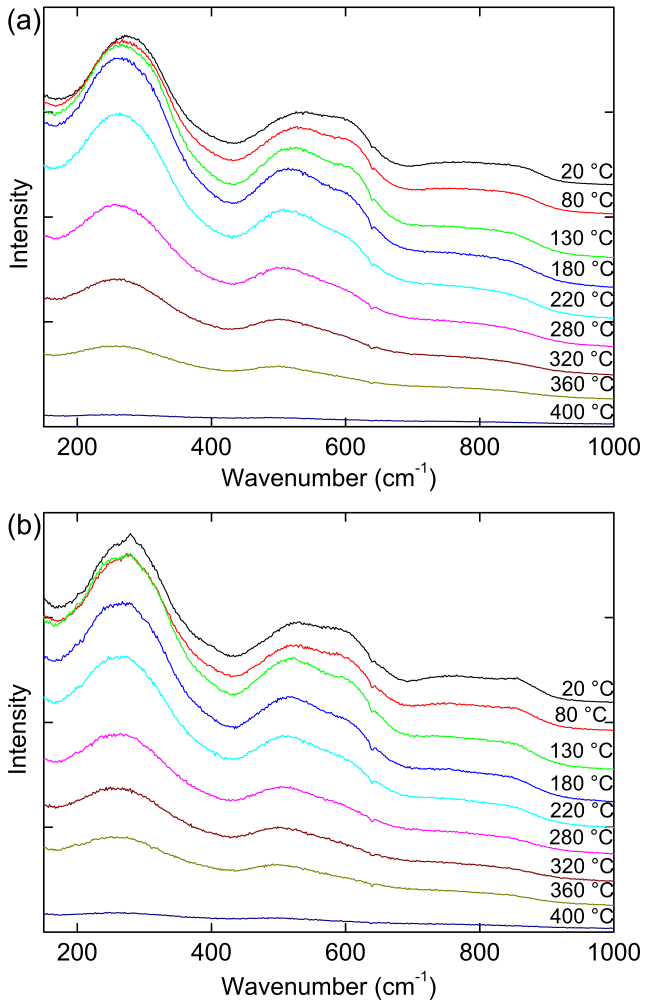

FIG. 7. Raman spectra obtained on heating for (a) 0BZT and (b) 2BZT ceramics. The spectra are offset vertically for clarity.

A strong increase in I_{SH} due to increasing particle size has been observed in both quartz and $(NH_4)H_2PO_4$ (ADP),[39] but aspects of this behaviour depend on whether the material has a direction which is phase-matchable—where the fundamental and second harmonic waves travel at the same speed in a particular direction, allowing the second harmonics to constructively interfere. In a non-phase-matchable material such as quartz, I_{SH} reaches a peak when the mean particle size is equal to l_c, but falls as the particle size continues to increase. In a phase-matchable material such as ADP, I_{SH} saturates at a peak value for particle sizes above ~5l_c. In the 0BZT and 2BZT ceramics, the grain size is known to be ~1 μm,[24] close to the expected value of l_c, imposing a limit on the maximum size of the poled regions. The dependence of I_{SH} on electric field observed for 2BZT (Fig. 5(b)) reaches a maximum at a field strength of 3 kV mm^{-1}, with the slight reduction in I_{SH} for higher poling fields pointing towards a non-phase-matchable material like NBT.[16] Irrespective of whether the material is phase-matchable or not, the size of the poled regions must be of the order of l_c in the fully poled material. The effective particle size has therefore increased from a value estimated to be around a few nm, by ~2 orders of magnitude.[5,50] I_{SH} for 0BZT reaches a maximum value at a higher applied field, ≥5 kV mm^{-1}, indicating that 0BZT has a higher l_c than 2BZT. I_{SH} for 2BZT reaches its maximum value after poling in the region 2.5–3 kV mm^{-1}, significantly lower than its coercive field (3.5 kV mm^{-1}).[24] This indicates that the size of the poled regions has reached l_c and is further evidence that I_{SH} depends on the size of the poled regions and not directly on the sample polarisation.

On heating above T_F, switching of dipoles leads to shrinking of the poled regions, causing the effective particle size to reduce. The temperature when I_{SH} begins to fall most steeply is associated with this shrinking of poled regions, therefore indicating $T_F = 95(5)$ °C for 0BZT and $T_F = 130(5)$ °C for 2BZT (Fig. 5). At temperatures $<T_F$, the gradual reduction of I_{SH} on heating cannot be unambiguously linked to a reduction in the size of the poled regions. The effective T_F of ceramics poled at <3 kV mm^{-1} appears significantly lower than T_F of the same materials poled at ≥3 kV mm^{-1}, most clearly shown by the 2BZT sample poled

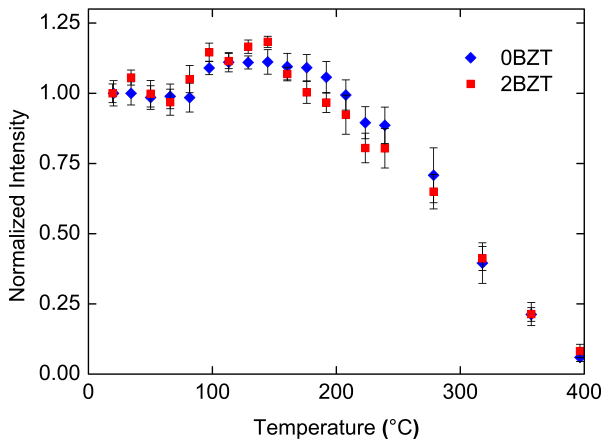

FIG. 8. Integrated intensity of the transverse optic A_1 mode at ~520 cm^{-1} for 0BZT and 2BZT ceramics.

at $2.5\,kV\,mm^{-1}$ (Fig. 5(b)), suggesting that T_F can be dependent on the magnitude of the poling field. The data in Fig. 6 demonstrate that the majority of depoling in 0BZT takes place between 120 and 125 °C—a significantly higher temperature than T_d (103 °C, Fig. 2).

None of the prior studies where SHG was performed on relaxors have addressed the effect of zero-field heating on poled samples. The field-cooled SHG data from $Li_xK_{(1-x)}TaO_3$ relaxors[36,37] do not exhibit such clear saturation of I_{SH} and require a much shorter temperature range (~20–40 °C) to go from minimum to maximum values. This may be connected with the fact that the Li-based samples are heated and cooled under an applied field, or that the poled regions have not reached a size comparable with the crystals. The SHG data from $Li_xK_{(1-x)}TaO_3$ appear much more similar to data obtained from a classical ferroelectric (e.g., Ref. 42). SHG data obtained from the unpoled Bi-based samples display no changes on cooling or heating through the region of T_F, unlike PLZT 8/65/35 (Ref. 32) and $Pb(Mg_{2/3}Nb_{1/3})O_3$-based materals.[34] The reasons for this are unclear, but it may be that evidence of a transition around T_F is seen only when there are remnant electric fields or stresses present.[51]

The SHG data in Fig. 5 indicate that the poled regions shrink and disappear across the temperature range 95–160 °C in 0BZT and 130–230 °C in 2BZT. Across this range, the microstructure gradually transforms from that of the field-induced ferroelectric to the ergodic relaxor in an unfreezing process that is clearly not instantaneous.[8] Within this temperature range, the poled regions are static and larger than in an annealed sample and the microstructure is not in its equilibrium state. Some dependence of this temperature range on the heating rate is to be expected. Above these temperature ranges, the poled and unpoled materials are indistinguishable from each other and the effects of the poling field have been fully removed. On cooling back to room temperature, I_{SH} increases, though not to the level observed in the poled material, due to the PNRs increasing in size during cooling. The integrated Raman intensities in Fig. 8 show a small but repeatable increase at 90(10) °C that could be associated with a release of internal stresses on approaching T_d. Between the temperatures 95–145 °C, the intensity is maximised, indicating that T_F is located within this range for both materials.[46,47] However, as the coherence length in Raman spectroscopy is expected to be only a few nm and therefore around 2 orders of magnitude less than that of SHG, it can be concluded that the phenomenon at T_F is short-range and that on an atomic scale there is very little change in the material as it loses its macroscopic polarisation. At $T_B \sim 400$ °C, the PNRs finally disappear.[46]

SHG is shown to be extremely useful for (a) locating the relaxor—induced ferroelectric structural change arising from poling or field-cooling, (b) indicating the temperature range over which the poled regions shrink through the transition from field-induced ferroelectric to ergodic relaxor and (c) obtaining indicative values of T_d and T_F.

XRD reveals the presence of both rhombohedral and pseudocubic materials. Relaxors are known to have significant lattice disorder that can result in bulk diffraction techniques showing a higher symmetry than is present on a local scale,[52] as has also been observed in the classical ferroelectric PZT.[53] Therefore, starting from the assumption that, on a unit cell level, all of the material is rhombohedral with a corresponding dipole vector, the rhombohedral material observed by XRD arises from the poled regions and can be considered as no different from a classical rhombohedral ferroelectric: it appears rhombohedral in XRD, it has a net polarisation and produces a second harmonic. The pseudocubic material therefore arises from the non-polar matrix in which the individual unit cells are polar, but neighbouring unit cells have randomly oriented dipole vectors. These regions appear cubic in XRD, have no net polarisation and do not produce a second harmonic. The process of poling transforms the pseudocubic material into rhombohedral material by simply aligning the dipoles. The thermal depoling process therefore does not require a change in symmetry on a unit cell level, nor the presence of an antiferroelectric phase in order to be consistent with observations.[54]

Some variation exists between the values of transition temperature (T_d or T_F) determined by different techniques (Table I). This has been observed before in Bi-based relaxors[9] and has been rationalised by the existence of two different mechanisms by which the poled material can lose its polarisation; domain reorientation followed by domain break-up into PNRs. It is also important to note that these techniques probe different characteristics of the crystal structure and have quite different interaction lengths with the material under investigation. The results from Raman spectroscopy are not included in this table as they show a far smaller change when compared with the other techniques.

In a classical ferroelectric phase transition, strain, polarisation, and I_{SH} would be expected to change sharply at the same temperature, since in the model of the displacive phase transition, these variables are inextricably linked through a single mechanism—a sample-wide, correlated realignment or loss of the unit cell dipole vectors. In a relaxor material, the transition between field-induced ferroelectric and ergodic relaxor can take place with two different switching mechanisms

(a) Correlated switching: Groups of unit cells change dipole vectors together in a manner similar to twinning. With underlying rhombohedral symmetry, this allows switching to occur through angles of 71°, 109°, or 180°, in order of increasing effect on the macroscopic polarisation.
(b) Uncorrelated switching: Individual unit cells change dipole vectors in a random fashion and without correlation to their nearest neighbours, generating material

TABLE I. Transition temperatures for the two samples as determined by different techniques.

	0BZT	2BZT
TSDC	103(1) °C	119(1) °C
XRD	95(2) °C	115(2) °C
SHG	95(5) °C	130(5) °C

which, on average, appears cubic. This can grow the pseudocubic region at the expense of the rhombohedral areas, reducing the mean size of the poled regions, or "swallow up" the smaller polar regions and thereby reduce their number.

Evidence for more than one depolarisation mechanism can be seen in other experiments. Pinched polarisation hysteresis loops such as those observed in NBT-based materials demonstrate that relaxors that are poled by an external electric field partially depole themselves as the field is removed at temperatures well below T_F.[55] The involvement of multiple mechanisms means that different techniques may show their greatest change at different temperatures. For example, correlated switching can result in macroscopic polarisation loss without the appearance of pseudocubic material and without loss of SHG. Table II details the predicted effects on structure, macroscopic polarisation, and I_{SH} of the different switching mechanisms.

The data in Table I show that, for 2BZT, XRD indicates a change to a predominantly pseudocubic structure at a higher temperature than the depolarisation current. From Table II, this can be interpreted as the onset of correlated switching at a lower temperature than uncorrelated switching. In the materials studied by Anton *et al.*[9] and Sapper *et al.*,[13] it was found that using dielectric permittivity to measure T_d(dielectric) gave a temperature that was consistently higher than T_d obtained by other methods, including TSDC, piezoelectric resonance, and *in-situ* d_{33}. T_d(dielectric) was assigned to the inflection point in the plot of the real part of permittivity vs. temperature above which frequency dispersion associated with relaxor behaviour is observed. This can be interpreted as the ferroelectric–relaxor transition at T_F. Observing $T_F > T_d$ can be interpreted as evidence that correlated switching occurs at a lower temperature than uncorrelated switching.

The XRD data for 0BZT show the structural transition taking place at a lower temperature than the polarisation loss. This result was found to be repeatable, but stands in contrast not only to the XRD data for 2BZT but also for a recent study on NBT-KBT-KNN (Ref. 9), which demonstrated that T_d obtained by XRD is measured at a higher temperature than other methods. This peculiar result may indicate the onset of uncorrelated switching at a lower temperature than correlated switching, or the existence of more complex depolarisation mechanisms.

A model is presented for the cycle of polarisation and thermal depolarisation of relaxor ferroelectrics that is consistent with the data for 2BZT (Table I) and samples in other studies.[9,13,15]

The unpoled relaxor contains PNRs with randomly oriented polarisation in a matrix of non-polar material (Fig. 9(a)). Application and removal of an electric field causes alignment of almost all individual dipoles, resulting in the formation of poled regions at the expense of the non-polar material, to become analogous with domains in a classical ferroelectric (Fig. 9(b)). On heating to a temperature in the region of T_d, correlated switching commences, causing rapid loss of macroscopic polarisation (Fig. 9(c)). On heating to $\sim T_F$, uncorrelated switching becomes the dominant mechanism. The non-polar material containing dynamic PNRs grows and the static, poled regions shrink (Fig. 9(d)). On further heating to a temperature in excess of T_F but below T_B, all static poled regions have gone. Individual dipoles reduce in magnitude as the material approaches its cubic phase and PNRs continue to shrink (Fig. 9(e)). Further heating leads to the disappearance of the PNRs at T_B.

TABLE II. Summary of the effects of different polarisation switching mechanisms on measurable properties for a rhombohedral relaxor material.

	Switching Mechanism	
Property	Correlated Switching	Uncorrelated Switching
Structure	Stays rhombohedral	Becomes pseudocubic
Polarisation	Reduces (71°/109°/180° domains)	Reduces (locally averaged dipole)
I_{SH}	Falls to non-zero intensity	Falls to zero

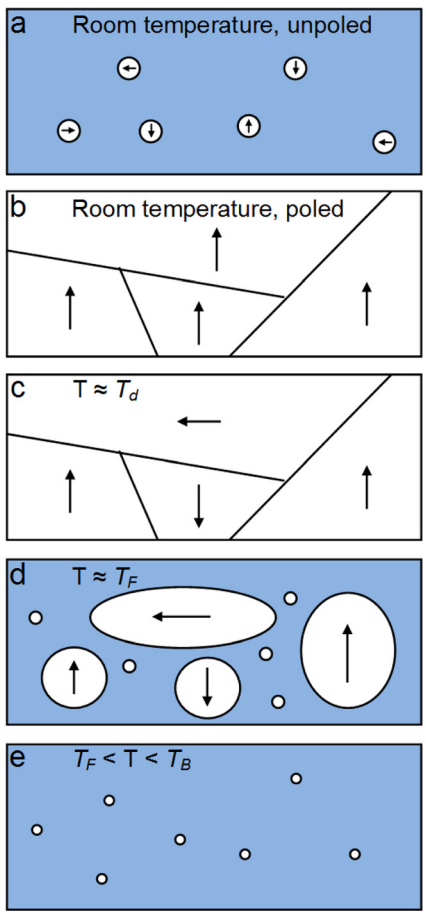

FIG. 9. Illustration of key stages in the depolarisation mechanism. Blue areas represent non-polar (pseudocubic) material, white areas represent polar (rhombohedral) material, and arrows represent direction and magnitude of static polarisation. Images are not intended to be at the same scale. (a) Room temperature, unpoled; non-ergodic relaxor. PNRs in pseudocubic matrix, (b) Electric field applied and removed. Aligned domains with rhombohedral structure, (c) $T \approx T_d$: Correlated switching of domains reduces macroscopic polarisation, (d) $T \approx T_F$: Uncorrelated switching reduces size of static poled regions and increases proportion of pseudocubic phase containing dynamic PNRs, (e) $T_F < T < T_B$: Dynamic PNRs continue to shrink.

The different rhombohedral distortions for the two materials, as shown in Figs. 3 and 4, lead to a hypothesis for the increased T_d in 2BZT. It is suggested that the addition of BZT increases the strength of neighbouring dipole-dipole interactions, raising T_d, but also shifts the location of the phase boundary in NBT-KBT in a manner similar to how additions of KNN have been found to shift the phase boundary in NBT-$BaTiO_3$.[56]

V. CONCLUSIONS

Second harmonic generation, thermally stimulated depolarisation current, Raman spectroscopy, and X-ray diffraction have been used to investigate the thermal depolarisation of poled $(Na_{0.8}K_{0.2})_{1/2}Bi_{1/2}TiO_3$ ceramics with and without doping by $BiZn_{1/2}Ti_{1/2}O_3$ as examples of lead-free relaxor ferroelectrics.

Second harmonic generation performed on samples fully poled by an electric field shows (i) on poling, a significant increase in second harmonic intensity, corresponding to an increase in the size of poled regions by ~2 orders of magnitude, (ii) on heating, a steep decrease in intensity that commences at the freezing temperature, T_F, and (iii) that the transition from field-induced ferroelectric to equilibrium ergodic relaxor takes place across a temperature range of ~100 °C. Ceramics in all stages of polarisation appear isotropic with respect to second harmonic generation.

Each of the techniques used provided a different measure of the macroscopic depolarisation temperature, T_d. This is explained by the concept of correlated and uncorrelated dipole switching, providing more than one mechanism for depolarisation, each of which has differing effects on measurable quantities.

A model of the field- and temperature-induced changes within a relaxor is described that explains the observations. On a unit cell level, there is no necessity for a phase transition to take place during depolarisation.

ACKNOWLEDGMENTS

This work was supported by EPSRC grant number EP/G02586X/1. R.D., W.J., and J.R. were supported by the Deutsche Forschungsgemeinschaft (DFG) under SFB595. D.S.K. thanks the Science City Research Alliance and the HEFCE Strategic Development Fund for financial support.

The PANalytical MPD diffractometer used in this research was obtained through the Science City Energy Futures Project: Hydrogen Energy, with support from Advantage West Midlands (AWM).

[1]C.-S. Tu, I. G. Siny, and V. H. Schmidt, Phys. Rev. B **49**, 11550 (1994).
[2]W. Jo, R. Dittmer, M. Acosta, J. Zang, C. Groh, E. Sapper, K. Wang, and J. Rödel, J. Electroceram. **29**, 71 (2012).
[3]G. Burns and F. H. Dacol, Solid State Commun. **48**, 853 (1983).
[4]D. Viehland, S. J. Jang, L. E. Cross, and M. Wuttig, J. Appl. Phys. **68**, 2916 (1990).
[5]G. Xu, G. Shirane, J. R. D. Copley, and P. M. Gehring, Phys. Rev. B **69**, 064112 (2004).
[6]G. A. Samara, J. Phys.: Condens. Matter **15**, R367 (2003).
[7]V. V. Shvartsman and D. C. Lupascu, J. Am. Ceram. Soc. **95**, 1 (2012).
[8]A. A. Bokov and Z.-G. Ye, J. Mater. Sci. **41**, 31 (2006).
[9]E.-M. Anton, W. Jo, D. Damjanovic, and J. Rödel, J. Appl. Phys. **110**, 094108 (2011).
[10]M. Davies, E. Aksel, and J. L. Jones, J. Am. Ceram. Soc. **94**, 1314 (2011).
[11]J. Toulouse, B. E. Vugmeister, and R. Pattnaik, Phys. Rev. Lett. **73**, 3467 (1994).
[12]B. E. Vugmeister, Phys. Rev. B **73**, 174117 (2006).
[13]E. Sapper, S. Schaab, W. Jo, T. Granzow, and J. Rödel, J. Appl. Phys. **111**, 014105 (2012).
[14]W. Ge, D. Maurya, J. Li, S. Priya, and D. Viehland, Appl. Phys. Lett. **102**, 222905 (2013).
[15]W. Jo, J. Daniels, D. Damjanovic, W. Kleemann, and J. Rödel, Appl. Phys. Lett. **102**, 192903 (2013).
[16]G. O. Jones and P. A. Thomas, Acta Cryst. B **58**, 168 (2002).
[17]A. O'Brien, D. I. Woodward, K. Sardar, R. I. Walton, and P. A. Thomas, Appl. Phys. Lett. **101**, 142902 (2012).
[18]E. Aksel, J. S. Forrester, B. Kowalski, M. Deluca, D. Damjanovic, and J. L. Jones, Phys. Rev. B **85**, 024121 (2012).
[19]S. Gorfman, A. M. Glazer, Y. Noguchi, M. Miyayama, H. Luod, and P. A. Thomas, J. Appl. Cryst. **45**, 444 (2012).
[20]C. Ma, X. Tan, E. Dul'kin, and M. Roth, J. Appl. Phys. **108**, 104105 (2010).
[21]A. Sasaki, T. Chiba, Y. Mamiya, and E. Otsuki, Jpn. J. Appl. Phys., Part 1 **38**, 5564 (1999).
[22]M. Otoničar, S. D. Škapin, M. Spreitzer, and D. Suvorov, J. Eur. Ceram. Soc. **30**, 971 (2010).
[23]Y. Hiruma, H. Nagata, and T. Takenaka, J. Appl. Phys. **104**, 124106 (2008).
[24]R. Dittmer, W. Jo, J. Daniels, S. Schaab, and J. Rödel, J. Am. Ceram. Soc. **94**, 4283 (2011).
[25]O. Elkechai, M. Manier, and J. P. Mercurio, Phys. Status Solidi A **157**, 499 (1996).
[26]M. R. Suchomel, A. M. Fogg, M. Allix, H. J. Niu, J. B. Claridge, and M. J. Rosseinsky, Chem. Mater. **18**, 4987 (2006).
[27]T. Takenaka, K. Maruyama, and K. Sakata, Jpn. J. Appl. Phys., Part 1 **30**, 2236 (1991).
[28]G. New, *Introduction to Nonlinear Optics* (Cambridge University Press, 2011).
[29]Y. R. Shen, *The Principles of Nonlinear Optics* (Wiley, New Jersey, 2003).
[30]J. P. Dougherty and S. K. Kurtz, J. Appl. Cryst. **9**, 145 (1976).
[31]S. A. Denev, T. T. A. Lummen, E. Barnes, A. Kumar, and V. Gopalan, J. Am. Ceram. Soc. **94**, 2699 (2011).
[32]K. Betzler and D. Bäuerle, Appl. Phys. **18**, 271 (1979).
[33]M. Pavel, I. Rychetský, P. Kužel, and M. Kosec, Ferroelectrics **238**, 291 (2000).
[34]K. Fujishiro, T. Iwase, Y. Uesu, Y. Yamada, B. Dkhil, J.-M. Kiat, S. Mori, and N. Yamamoto, J. Phys. Soc. Jpn. **69**, 2331 (2000).
[35]J. Kroupa, V. Bovtun, D. Nuzhnyy, M. Savinov, P. Vanek, S. Kamba, J. Petzelt, J. Holc, M. Kosec, H. Amorín, and M. Alguero, Phase Trans. **81**, 1059 (2008).
[36]H. Yokota, T. Oyama, and Y. Uesu, Phys. Rev. B **72**, 144103 (2005).
[37]H. Yokota, Y. Uesu, C. Malibert, and J.-M. Kiat, Phys. Rev. B **75**, 184113 (2007).
[38]D. V. Isakov, T. R. Volk, and L. I. Ivleva, Phys. Solid State **51**, 2334 (2009).
[39]S. K. Kurtz and T. T. Perry, J. Appl. Phys. **39**, 3798 (1968).
[40]*Handbook of Chemistry and Physics*, edited by W. M. Haynes (CRC Press, Boca Raton, 2011).
[41]N. Masó, D. I. Woodward, P. A. Thomas, A. Várez, and A. R. West, J. Mater. Chem. **21**, 2715 (2011).
[42]K. Datta, P. A. Thomas, and K. Roleder, Phys. Rev. B **82**, 224105 (2010).
[43]J. Kreisel, A. M. Glazer, G. Jones, P. A. Thomas, L. Abello, and G. Lucazeau, J. Phys: Condens. Matter **12**, 3267 (2000).
[44]B. Wylie-van Eerd, D. Damjanovic, N. Klein, N. Setter, and J. Trodahl, Phys. Rev. B **82**, 104112 (2010).
[45]J. Kreisel, A. M. Glazer, P. Bouvier, and G. Lucazeau, Phys. Rev. B **63**, 174106 (2001).
[46]A. Kumar, I. Rivera, and R. S. Katiyar, J. Raman Spectrosc. **40**, 459 (2009).
[47]R. Farhi, M. El Marssi, A. Simon, and J. Ravez, Eur. Phys. J. B **9**, 599 (1999).

[48]M. S. Islam, S. Tsukada, W. Chen, Z.-G. Ye, and S. Kojima, J. Appl. Phys. **112**, 114106 (2012).
[49]M. Bousquet, J.-R. Duclère, E. Orhan, A. Boulle, C. Bachelet, and C. Champeaux, J. Appl. Phys. **107**, 104107 (2010).
[50]R. Dittmer, W. Jo, J. Rödel., S. Kalinin, and N. Balke, Adv. Funct. Mater. **22**, 4208–4215 (2012).
[51]C. Michel and A. Sicignano, Appl. Phys. Lett. **24**, 559 (1974).
[52]W. Kleemann, J. Mater. Sci. **41**, 129 (2006).
[53]A. M. Glazer, P. A. Thomas, K. Z. Baba-Kishi, G. K. H. Pang, and C. W. Tai, Phys. Rev. B **70**, 184123 (2004).
[54]W. Jo, S. Schaab, E. Sapper, L. A. Schmitt, H.-J. Kleebe, A. J. Bell, and J. Rödel, J. Appl. Phys. **110**, 074106 (2011).
[55]S.-T. Zhang, A. B. Kounga, E. Aulbach, W. Jo, T. Granzow, H. Ehrenberg, and J. Rödel, J. Appl. Phys. **103**, 034108 (2008).
[56]S.-T. Zhang, A. B. Kounga, E. Aulbach, T. Granzow, W. Jo, H.-J. Kleebe, and J. Rödel, J. Appl. Phys. **103**, 034107 (2008).